Inverse spin Hall effect in heterostructures "nanostructured ferromagnet/topological insulator"

P.N. Petrov[1,*], *M.D.* Davydova[1], *P.N.* Skirdkov[1,2,3], *K.A.* Zvezdin[1,2,3], *J.G.* Lin [4], *J.C.A.* Huang[5]

[1] Moscow Institute of Physics and Technology, 141700 Dolgoprudny, Russia
[2] Russian Quantum Center, 143025 Skolkovo, Moscow Region, Russia
[3] A.M. Prokhorov General Physics Institute, RAS, 119991 Moscow, Russia
[4] National Taiwan University, Taipei, 106 Taiwan, Republic of China
[5] National Cheng Kung University, Tainan, 701 Taiwan, Republic of China

Abstract. Interaction between magnetization dynamics and spin polarized electronic transport has been studied for ferromagnet nanodisk situated upon a 3D topological insulator (TI) film. Resonant magnetization dynamics leads to generation of spin current, which flows into the topological insulator, where spin to charge conversion occurs. Using micromagnetic simulations for magnetization dynamics we estimate the dc voltage, which is created due to this process in topological insulator. Contribution from different modes, which are characteristic for nanodisks, to the voltage was calculated.

1 Introduction

Interaction between magnetization dynamics and spin polarized electronic transport has been first studied by Slonczewski [1] and Berger [2]. It has been predicted and later experimentally proven that the spin polarized current can drive magnetization dynamics via a spin torque mechanism, and that in an inverse process, resonant magnetization dynamics can lead to generation of spin current which is related to the spin pumping mechanism [3]. When spin polarized current flows into the material with strong spin-orbit interaction, the spin-to-charge conversion takes place. One of the possible mechanisms of such conversion is inverse spin Hall effect (ISHE) [4,5], which occurs in volume, and the other is the inverse Rashba-Edelstein effect (IREE) [5], connected with the spin-momentum locking for surface currents. We consider the heterostructure with thin metallic ferromagnet situated upon the topological insulator film. Due to the ferromagnet layer the bulk conductance in TI may be restored and the origin of the charge current in the experiment often lies in ISHE [6,7]. We consider the dc voltage, which arises in the system due to such mechanism. On the other hand, in work by Wang *et al.* [8] in YIG-TI bilayers with Bi_2Se_3 the IREE effect was found to be dominant over ISHE (the assumption of negligence of ISHE mechanism was made due to the smallness of the fitted spin diffusion length λ_{SD}). However, the interface between metallic FM like Py and nonmetallic YIG and TI may have very different properties, which may explain the discrepancy in the experimental results.

Recently, spin pumping and dc voltage generation was studied in bilayer systems with metallic ferromagnet and three-dimensional topological insulator Bi_2Se_3 at room temperature [7], which has proved the possibility of efficient spin-to-charge conversion in such systems. Three-dimensional (3D) topological insulators are known for their strong spin-orbit coupling and the existence of spin-textured topological surface states which could be potentially used for spintronics applications. The measure of the spin-to-charge conversion rate in considered mechanism corresponds to spin Hall angle θ_{SH}, which for Bi_2Se_3 has the giant value, equal to 0.38 [9], which makes it a perfect candidate material for topological spintronics [10].

We consider structure, which consists of a ferromagnetic (FM) nanodisk with diameter either 200 or 400 nm and thickness 4 nm, which is situated upon the 50 nm thick topological insulator film, as shown in Fig. 1. The necessity for investigation of nanostructured system is connected with the need for miniaturization of future spintronic devices. It is known that in structured ferromagnets shape modes arise [11], which have been studied previously [12]. The existence of additional modes comparing to sheet film structures opens a possibility for frequency tuning and increasing the number of varying parameters in the system, which may be important for practical applications. Moreover, such structures can be arranged into 2D arrays, in which coupling occurs and new properties arise [13].

In this work we use micromagnetic modelling to study properties of spin pumping in heterostructures, consisting of FM nanodot upon a topological insulator.

* Corresponding author: petr.petrov@phystech.edu

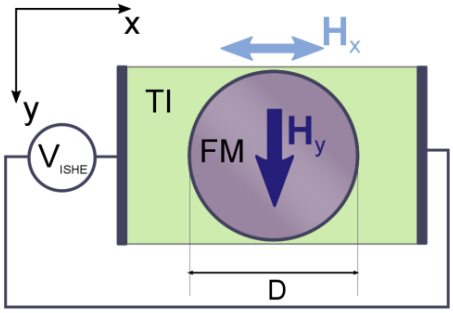

Fig. 1. Schematic structure of the considered bilayer system. D = 200/400 nm denotes the diameter of the ferromagnet nanodisk and V_{ISHE} is the measured dc current due to spin pumping from ferromagnetic resonance in ferromagnet.

We use permalloy (FM) and Bi_2Se_3 (TI) as modelling materials. Short investigation of the sensitivity of the second ('end') mode on the ferromagnet properties, such as exchange constant, g-factor and net magnetization was performed. We then calculate spin current density in each cell and obtain dc voltage due to spin-to-charge conversion. The second mode reveals itself as an additional peak in calculated dc voltage. Such peak was not observed in recent experimental results with spin pumping between dielectric ferromagnet and bismuth selenide [8] but seen clearly in experiments on ferromagnetic resonance in permalloy nanodisks [14].

2 Micromagnetic modelling and ISHE voltage

Magnetization dynamics in the nanodisk is caused by the ferromagnetic resonance in the presence of large constant in-plane magnetic field H_y, which is applied along y-axis (see Fig. 1), and a small oscillating perpendicular in-plane component H_x. The magnetization dynamics was obtained using our micromagnetic finite-difference code 'SpinPM', which is based on the fourth-order Runge-Kutta method with an adaptive timestep control for the time integration and mesh size of 2.5 nm × 2.5 nm × 4 nm..

The results for the average net magnetization of the nanodisk with D = 200 nm with enhanced Gilbert damping $\alpha = 0.0275$ (this damping corresponds to effective spin-mixing constant g^{eff} at the interface, equal to 3.7×10^{19} m^{-2}, which is characteristic value for similar heterostructures [7]) taken into account are shown in Figs. 2 and 3. Enhanced Gilbert damping, which can be expressed as $\Delta\alpha = \left(g\mu_B g^{eff}\right)/\left(4\pi M_S h_{FM}\right)$ (h_{FM} is the thickness of the ferromagnetic layer, M_S is the saturation magnetization) is the result of angular momentum transfer from ferromagnet into attached layer of nonmagnetic material [15].

The results for micromagnetic simulations of *x*- and *z*- components of magnetization are shown in Figs. 2a and 2b. The *y*-component is approximately equal to saturation magnetization due to strong bias magnetic field in this direction.

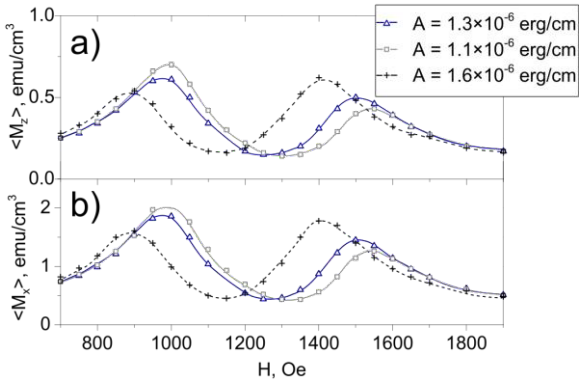

Fig. 2. Dependence of average in period for a) – *x*-component and b) – *z*-component of net magnetization in nanodisk with D = 200 nm for different exchange constants on bias magnetic field. M_s = 800 emu/cm^3, g = 2. Lines are guides to the eyes.

In Fig. 2 dependence of the behavior of both resonance peaks on the exchange constant in ferromagnet is illustrated. The lower field mode corresponds to Kittel homogeneous resonance, whereas the higher mode is 'end' mode investigated in ref. [14]. However, the behavior of this mode in presence of varying material parameters was not considered there due to absence of analytical investigations, which is also an important question from practical point of view, which we address for further thorough research. Here we provide only a short insight into the problem. As it is seen from Fig. 2, the distance between the two peaks remains almost constant, whereas ratio of resonance height varies a lot depending on the exchange constant.

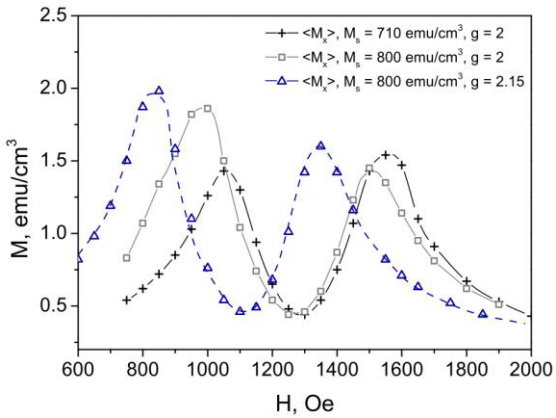

Fig. 3. Dependence of average in period net magnetization in nanodisk with D = 200 nm for different saturation magnetizations and g-factor on bias magnetic field. Exchange constant is taken to be A = 1.3×10^{-6} erg/cm. Lines are guides to the eyes.

In Fig. 3 the ferromagnetic resonance is simulated for different saturation magnetizations and different g-factors, which are the parameters which also vary between different experiments for the same materials. The homogeneous resonant peak is naturally sensitive to the saturation magnetization, whereas 'end' mode is much less sensitive, which may allow additional method for controlling their ratio.

The magnetization dynamics data with enhanced Gilbert damping taken into account was used to obtain

spin current flow due to spin pumping in each cell. According to the conventional spin pumping theory spin current appears as a result of oscillations of chemical potential in nonmagnetic layer [15]. It was shown that bulk ISHE pumping signal may be described with the same expressions as in theory for the ferromagnet-normal metal systems [16]. However, it is important to note that the material coefficients in the theory are effective constants with difference, which lies in large spin orbit coupling on the FM-TI interface. The spin current density flow to the TI in *z*-direction (perpendicular to the interface) is expressed in the following way:

$$(\mathbf{j}_s)_z = \frac{\hbar}{4\pi} g^{eff} \left[\mathbf{m}, \frac{d\mathbf{m}}{dt} \right], \quad (1)$$

where g^{eff} is the effective spin-mixing constant, $\mathbf{m}$ is unit magnetization vector in the current cell and the vector components $\mathbf{j}_z$ correspond to spin polarization. Equation (1) describes the spin current at the interface, whereas in the bulk it decays according to [16]:

$$\mathbf{j}_s(z) = \mathbf{j}_s(0) \sinh\left(\frac{h-z}{\lambda_{SD}} \right) / \sinh\left(\frac{h}{\lambda_{SD}} \right), \quad (2)$$

where h is the thickness of the TI film and $\lambda_{SD} \approx 6$ nm is the spin diffusion length in Bi_2Se_3. Due to the inverse spin Hall effect in TI the spin current flow gives the rise to charge current using empirical spin Hall angle parameter θ_{SH} [17]:

$$\mathbf{j}_c = \frac{2e}{\hbar} \theta_{SH} \left[j_s \mathbf{e}_z, \boldsymbol{\sigma} \right]. \quad (3)$$

Here we take that inverse to spin Hall effect process is reciprocal in terms of the spin-to-charge conversion constant $\theta_{SH} \approx 0.4$, which lies in agreement with experimental results [7,17], and $\boldsymbol{\sigma}$ is the polarization of the spin current.

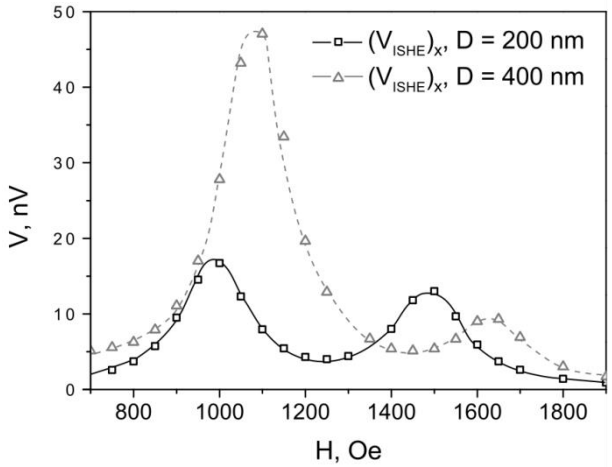

Fig. 4. Dependence of dc ISHE voltages in nanodisks with D = 200 nm and D = 400 nm in x-direction on bias magnetic field at parameters M_s = 800 emu/cm^3, g = 2, A = 1.3×10^{-6} erg/cm. Lines are guides to the eyes.

Finally, the voltage, which is found on the edges of topological insulator due to the charge current flow, can be expressed as

$$V_{ISHE} = \langle j_c \rangle SR = \langle j_c \rangle DhR, \quad (4)$$

where R is the resistance of the film in x-direction, which we take to be roughly equal to 240 Ω [18]. The average spin current polarization is nonzero for *y*-direction and from the structure of eq. (3) it is seen that the voltage will arise in *x*-direction. The results for the *x*-components of ISHE voltage calculations are present in Fig. 4. The peak values of this dc voltage are approximately equal to 47 nV for 400 nm disk and 17 nV for 200 nm disk, which is consistent with results from experiments with sheet films [6,7], if scaled.

The main difference between voltage in such nanostructure from sheet samples is that the existence of the second peak (see Fig. 4). It is seen from that input to the ISHE current from the 'end' mode is much smaller in comparison to homogeneous resonance in case of larger disk diameter, and in limit of sheet films this resonance will vanish [7]; whereas for smaller disks both peaks are approximately same in height. A resonance with lower frequency corresponds to the higher peak in terms of magnetic field, which will possibly provide frequency tunability for future prospective spintronic devices.

3 Conclusion

In conclusion, we have investigated the ISHE voltage in heterostructures, which consist of thin nanodisk, situated upon topological insulator film. Two resonances with respect to bias magnetic field were found and investigated. The ratio between the two resonances was shown to be sensitive to the properties of ferromagnet. Verification of the existence of this second resonance in ISHE voltage with respect to magnetic field and further study of ISHE in nanostructured systems is a matter for future experimental verification.

The grant RSF No.17-12-01333 is acknowledged.

References

1. Slonczewski, J. C., *J. Magn. Magn. Mater* **159**, 1-2 (1996).
2. Berger L., *Phys. Rev. B.* **54**, 9533 (1996).
3. Ando, K., Takahashi, S., Ieda, J., Kajiwara, Y., Nakayama, H., Yoshino, T., Harii, K., Fujikawa, Y., Matsuo, M., Maekawa, S. and Saitoh, E., *J. Appl. Phys.* **109**, 10, (2011).
4. Saitoh, E., Ueda M., Miyajima H., and Tatara G., *Appl. Phys. Lett.* **88**, 18 (2006)
5. Edelstein, V. M., *Solid State Commun*. **73**, 3 (1990)
6. Deorani, P., Son, J., Banerjee, K., Koirala, N., Brahlek, M., Oh, S. and Yang, H., *Phys. Rev. B* **90**, 9 (2014)

7. Jamali, M., Lee, J.S., Jeong, J.S., Mahfouzi, F., Lv, Y., Zhao, Z., Nikolić, B.K., Mkhoyan, K.A., Samarth, N. and Wang, J.P., *Nano Letters* **15**, 10 (2015)
8. Wang, H., Kally, J., Lee, J.S., Liu, T., Chang, H., Hickey, D.R., Mkhoyan, K.A., Wu, M., Richardella, A. and Samarth, N., *Phys. Rev. Lett.* **117**, 7 (2016).
9. Mellnik, A.R., Lee, J.S., Richardella, A., Grab, J.L., Mintun, P.J., Fischer, M.H., Vaezi, A., Manchon, A., Kim, E.A., Samarth, N. and Ralph, D.C., *Nature* **511**, 7510 (2014)
10. Wang, K.L., Lang, M. and Kou, X., *Handbook of Spintronics,* pp. 431-462. (2016)
11. Dillon Jr, J.F., 1960, *J. Appl. Phys.,* **31**, 9 (1960)
12. Shaw, J.M., Silva, T.J., Schneider, M.L. and McMichael, R.D., *Phys. Rev. B* **79**, 18 (2009)
13. Velten, S., Streubel, R., Farhan, A., Kent, N., Im, M.Y., Scholl, A., Dhuey, S., Behncke, C., Meier, G. and Fischer, P., *Appl. Phys. Lett.* **110**, 26 (2017)
14. Shaw, J.M., Silva, T.J., Schneider, M.L. and McMichael, R.D., *Phys. Rev. B* **79**, 18 (2009)
15. Tserkovnyak, Y., Brataas, A., Bauer, G.E. and Halperin, B.I., *Rev. Mod. Phys* **77**, 4 (2005)
16. Chen, K. and Zhang, S., *Phys. Rev. Lett.* **114**, 12 (2015)
17. Saitoh, E., Ueda, M., Miyajima, H. and Tatara, G., *Appl. Phys. Lett.* **88**, 18 (2006)
18. Stordeur, M., Ketavong, K.K., Priemuth, A., Sobotta, H. and Riede, V., *Phys. Status Solidi B* **169**, 2 (1992)